

# ON THE USE OF $\Lambda$ TRANSITIONS IN ATOMIC FREQUENCY STANDARDS

Filippo Levi\*, Aldo Godone\*, Salvatore Micalizio\*\*, and Jacques Vanier\*\*\*

\*Istituto Elettrotecnico Nazionale "G. Ferraris" (IEN),

Str. delle Cacce 91, 10135 Turino, Italy

\*\*Politecnico di Torino, C. so Duca degli Abruzzi 24, 10129 Torino, Italy

\*\*\*Dép. de physique, Un. de Montréal and Guest Professor at IEN

## Abstract

*The possibility of using a three-level- $\Lambda$ -scheme for the excitation of the clock hyperfine transition in  $^{87}\text{Rb}$  is analyzed. The physics involved opens up two distinct avenues useful for the implementation of an atomic frequency standard, avenues based on two distinct phenomena: the electro-magnetically induced transparency (EIT or Dark Line) and the coherent microwave emission (Maser without population inversion). In spite of the close connection between the two phenomena, which are generated by the coherence created in the ground state by means of two coherent laser radiation fields (Coherent Population Trapping), the characteristics of an atomic frequency standard based on either of these phenomena may be quite different. The paper discusses the possibility of implementing on the basis of these two phenomena, new  $^{87}\text{Rb}$  atomic frequency standards having an excellent frequency stability, and makes explicit their differences.*

## INTRODUCTION

The possibility of observing atomic hyperfine resonances by means of Coherent Population Trapping (CPT) has been known for many years [1], while microwave emission due to the creation of a coherence in the ground state by the same CPT phenomenon was discovered more recently [2-3]. The availability of laser diodes makes possible the implementation of atomic frequency standards based on either of these effects.

As will be described in more details in the next section, two laser radiation fields used in a  $\Lambda$  configuration, as shown in Figure 1, create a coherence in the ground state of the atomic system leading to an electro-magnetically induced transparency effect (EIT) in the optical domain. This EIT effect has its maximum when the frequency difference of the two laser radiation fields is equal to the hyperfine splitting of the atom ground state. This signal can be used for the implementation of a frequency standard. In that case the physical construction of the system is relatively simple because no microwave cavity is needed to excite the atomic microwave transition and the detection and servo systems are basically identical to those used in the classical optically pumped rubidium frequency standard.

In a previous paper, we have analyzed also the possibility of using the observed coherent microwave emission in the implementation of a new atomic frequency standard: the CPT-Maser [4]. This maser should have a frequency stability behavior somewhere between that of a classical rubidium frequency standard and a hydrogen maser. Its physical implementation may be more complex than a classical rubidium frequency standard, but simpler than a hydrogen maser. In fact, the physical packaging is not that different from a rubidium frequency standard one, while the electronics and the servo system are closer to those of a H-maser. Advantages and disadvantages of these different approaches are discussed

below.

## PHYSICS OF THE SYSTEM

### THEORY

A detailed analysis of the phenomenon of Coherent Population Trapping can be found in [3]. In the present paper, we will only summarize the results of interest. The dynamical behavior of the three-level system excited by means of two radiation fields may be described by the quantum mechanical Liouville equation:

$$\frac{\partial \rho}{\partial t} = \frac{1}{i\hbar} [H, \rho] \quad (1)$$

where  $\rho$  is a density matrix element and  $H$  is the interaction Hamiltonian and the square bracket represents the commutator operation of  $H$  and  $\rho$ . We assume that the two laser radiation fields have equal amplitudes and are resonant with the optical transitions. We also assume that the atoms are contained in a cell and that their motion is restricted by a buffer gas inhibiting transit times across the laser beam and Doppler effects at the ground state hyperfine frequency [5]. We call  $\omega_R$  the Rabi angular frequency of the optical excitation and assume that  $\omega_R \ll \Gamma^*$ , where  $\Gamma^*$  is the decay rate of atoms in the excited state, including the effect of spontaneous emission and collisions with the buffer gas atoms. The steady-state solution for the density matrix elements is:

$$\begin{aligned} \rho_{11} &= \rho_{22} \approx 1/2 \\ \rho_{33} &= \left( \frac{\omega_R}{\Gamma^*} \right)^2 \left( 1 - \frac{\omega_R^2}{\Gamma^*} \frac{\Gamma'}{\Gamma'^2 + \Omega_\mu^2} \right) \\ \rho_{12} &= \delta_{12} e^{i(\omega_1 - \omega_2)t} = -\frac{\omega_R^2}{2\Gamma^*} \frac{1}{\Gamma' + i\Omega_\mu} e^{i(\omega_1 - \omega_2)t} \end{aligned} \quad (2)$$

where the levels have been numbered as shown in Figure 1 from low to high energy.  $\rho_{11}$ ,  $\rho_{22}$  and  $\rho_{33}$  are the fractional populations of the ground-state levels,  $\Omega_\mu$  is the detuning between the two laser fields frequency difference,  $(\omega_1 - \omega_2)$ , and the atomic hyperfine transition,  $\Gamma' = \gamma_2 + \omega_R^2 / \Gamma^*$ ,  $\gamma_2$  being the relaxation rate of the coherence in the ground state. From this set of equations, it is evident that the population  $\rho_{33}$  of the excited level has a minimum when  $\Omega_\mu = 0$ . This effect creates a so-called Dark Line in the fluorescence spectrum. Furthermore, the coherence created in the ground state oscillates at the frequency difference between the two laser radiation fields. This oscillating coherence creates a magnetization  $\vec{M}$ , whose expectation value averaged over the atomic ensemble is

$$\langle \vec{M} \rangle = \text{Tr}(\vec{M}\rho) \quad (3)$$

Such an oscillating magnetization emits radiation at the frequency  $(\omega_1 - \omega_2)$  and represents the "source

term" in the field equation:

$$\nabla \times \nabla \times \vec{H} + \frac{1}{c^2} \frac{\partial^2 \vec{H}}{\partial t^2} = -\frac{1}{c^2} \frac{\partial^2 \vec{M}}{\partial t^2} \quad (4)$$

where  $\vec{H}$  is the oscillating magnetic field. Solving Equation (4) in terms of modes in a resonant microwave cavity, we obtain the power dissipated inside the cavity,  $P_D$ , and the power emitted by the atoms,  $P_a$ :

$$P_D = \frac{\omega_{21}\mu_0}{2Q_L} \int_{V_C} |\vec{H}(r)|^2 dV \quad (5)$$

$$P_a = \frac{1}{2V_C} \omega_{21}\mu_0\mu_B^2\eta Q_L N^2 |2\delta_{12}|^2 \quad (6)$$

Equation 6 describes the power emitted by the CPT maser and through equation (2), its line shape. The various terms in Equation 6 are defined as follows:  $V_C$  is the cavity volume,  $\mu_0$  and  $\mu_B$  are the vacuum permeability and the Bohr magneton respectively,  $\eta$  is the filling factor of the atomic ensemble in the cavity, and  $N$  is the number of atoms involved in the emission process.

The theory discussed is valid within the assumption that the optical transitions are not saturated and that the Rabi frequency associated with the microwave field generated by the atoms is small when compared to the resonance line width. When the Rabi frequency becomes large relative to the relaxation rates in the ground state, a situation achieved by increasing the cavity  $Q$ , the filling factor, or the number of atoms, the physics of the CPT maser undergoes several changes, which will be described in a future work [6].

## EXPERIMENTAL SETUP

The experimental setup is shown in Figure 2. A laser diode emitting at 794 nm, the wavelength of the  $D_1$  line of  $^{87}\text{Rb}$ , is frequency-modulated at one-half the hyperfine transition frequency, generating a series of sidebands separated from the carrier by multiples of 3.4 GHz. The laser beam, circularly polarized by means of  $\lambda/4$  retarder plate, is sent on a quartz cell containing the rubidium vapor and a buffer gas. The two first sidebands are in resonance with the two optical transitions at  $\omega_1$  and  $\omega_2$  and create, in the rubidium vapor, the phenomenon of Coherence Population Trapping and an associated ground state coherence. The quartz cell is placed inside a microwave cavity resonating in the  $TE_{011}$  mode at 6.8 GHz, the hyperfine frequency of  $^{87}\text{Rb}$ . A photodetector at the exit of the cavity detects the transmission of light by the rubidium vapor and is used to lock the laser frequency to the  $D_1$  absorption line of rubidium. The microwave emission is detected by means of a heterodyne receiver. A solenoid is used to create the magnetic field  $B_0$  along the laser beam direction, and provides the quantization axis. A set of high permeability magnetic shields is used to attenuate environmental magnetic field fluctuations. The setup shown allows also the observation of the Dark Line phenomenon at the photodiode detector situated at the exit of the cavity (bright line in that case since transmission is detected). In such a case the cavity can be detuned or conceptually removed without affecting the observed results.

In a laboratory bench setup it is standard practice to divide the laser beam into two beams: the first beam is used to servo the laser frequency on a rubidium cell and to monitor the modulation depth by means of a Fabry-Perot cavity used as an optical spectrum analyzer; the second beam is sent to the rubidium quartz cell stored inside the microwave cavity. This beam may be frequency tuned by means of an acousto-optic modulator for varying the frequency of excitation of the rubidium atoms. The modulator may also be used

as a switch for the analysis of the dynamical behavior of the atomic ensemble. This setup provides great flexibility for studying the frequency behavior of the rubidium ensemble under various excitation frequency conditions and under laser pulse conditions.

## MAIN SHIFT AND ASYMMETRY EFFECTS

In the following paragraphs we will examine some of the important phenomena which can affect the frequency of the CPT maser emission maximum and of the Dark Line minimum.

### THE LIGHT SHIFT

In first approximation and in the present method of excitation by means of sidebands of equal amplitudes, a laser frequency shift produces an equal displacement of the two ground state hyperfine levels, resulting in a net zero light shift. A deeper analysis, however, shows that this picture is far from being exact and that many others effects have to be considered. In fact, the light shift is zero only if we consider the linear light shift and if the two laser field (and the electric dipole coupling matrix elements) are equal. To be more precise, a frequency shift is introduced by the first sideband at  $\omega_1$  interacting with the other transition excited by the other sideband at  $\omega_2$ , and vice versa. The interactions do not cause real transitions, but nevertheless produce frequency shifts through virtual transitions. All the sidebands produced in the frequency modulation of the laser have a similar effect on the ground-state hyperfine levels. If the contributions of all these sidebands, as well as of the residual carrier, are taken properly into account, calculation shows that the total light shift  $\Delta\omega_{LS}$  is given by [7]:

$$\frac{\Delta\omega_{LS}}{\omega_{12}} = \left( \frac{\omega_{RL}}{\omega_{12}} \right)^2 \left\{ \Theta(m) + \xi(m) \left( \frac{\Delta_o}{\omega_{12}} \right)^2 \right\} \quad (7)$$

where  $m$  is the frequency modulation index,  $\Delta_o$  is the carrier detuning,  $\omega_{12}$  is the hyperfine angular frequency,  $\omega_R$  is the laser Rabi angular frequency.  $\Theta(m)$  and  $\xi(m)$  are parameters obtained in the calculation and are shown in Figure 3. It is observed that it is possible to minimize this light shift effect only with a proper choice of the modulation index  $m$ .

However, in practice, the two first sidebands can be made equal only to a certain degree, while the frequency tuning of the laser is kept under control only to a certain extent. If both a laser detuning  $\Delta$  and an imbalance of the two Rabi frequencies connected to the two optical transitions are introduced, it is observed experimentally that the minimum of the fluorescence (Dark Line) remains fixed while its shape becomes asymmetrical. At the same time if the spectrum emitted by the CPT maser is recorded, it is observed that the peak of the emission profile is shifted, while the line shape remains always symmetrical. The expression for  $\rho_{33}$ , providing the amplitude of the fluorescence and consequently the amplitude of the Dark Line, can be obtained by means of elementary algebra using Equation 1. However, the solution is rather complex and does not lead to easy interpretation. A numerical integration of Equation 1 shows that the minimum of  $\rho_{33}$  (Dark Line) is not affected by the detuning and imbalance of the laser radiation fields but its shape is distorted. On the other hand an analytical solution for  $\delta_{12}$  is readily obtained as:

$$\delta_{12} = -\frac{\omega_{R1}}{2\Gamma^*} \frac{(\Gamma^*/2)^2}{(\Gamma^*/2)^2 + \Delta_0^2} \frac{1}{\Gamma^* + i(\Omega_\mu + \Omega_{LS})}$$

with

(8)

$$\Omega_{LS} = \frac{(1-\beta^2)\omega_{R1}^2}{4} \frac{\Delta_0}{(\Gamma^*/2)^2 + \Delta_0^2}$$

where  $\beta = \omega_{R2}/\omega_{R1}$  is the ratio of the two Rabi frequencies associated with the two first sidebands. Figures 4 and 5 represent typical theoretical and experimental results.

An imbalance of 15% between the two sidebands and a laser detuning of 40 MHz produces an asymmetry of the order of 12 % in the dark line and an absolute frequency shift of 5 Hz of the maser emission maximum.

It is important to note that the Rabi frequencies involved in the definition of the parameter  $\beta$  include both the sidebands amplitude and the electric dipole coupling strength of the transitions involved. In fact, if the electric dipole matrix elements of the two optical transitions of the  $\Lambda$  scheme are not equal, the effect is the same as an imbalance in the sidebands amplitude. The dipole moments of the  $D_1$  and  $D_2$  transition for Cs and Rb are reported in Figure 6. It is evident that only the transition from  $S_{1/2}$  to  $P_{1/2}$  ( $D_1$ ) offers the required symmetry properties. Furthermore, the absence of a cycling transition is very important, because fluorescence from such a transition would reduce considerably the atomic coherence through direct incoherent optical excitation. The choice between Cs and Rb is then suggested by the greater signal available on the 0-0 transition in Rb due to the simpler Zeeman structure. The main effects related to the light shift are summarized in Table I [8].

EFFECT	DARK-LINE	CPT MASER
Linear light shift	absent	
Quadratic light shift	present ( $< 10^{-14}$ /MHz)	
Amplitude light shift	present but null at $m = 2, 4$	
Carrier detuning plus excitation asymmetry	asymmetry	shift

Table I – Main light shift effects in CPT frequency standards.

### THE CAVITY PULLING EFFECT

A major difference between the CPT maser and the Dark Line frequency standard is connected to the absence of a microwave cavity in the second case. This difference is not only relevant for practical implementation, but is also very important because of the cavity pulling effect present in the CPT maser. The atomic frequency shift as a function of the cavity detuning in the low power approximation can be written as

$$\Delta v_a = \left( \frac{Q_c}{Q_a} \right)^2 \Delta v_c$$

(9)

where  $\Delta v_a$  is the atomic emission frequency shift,  $\Delta v_c$  the cavity detuning,  $Q_c$  the cavity quality factor, and  $Q_a$  the atomic line quality factor. However, when the microwave field generated in the cavity is strong, stimulated emission may become important relative to the relaxation processes, causing a loss of coherence within the ground state. In such a case the cavity pulling effect becomes more significant and may eventually become nearly linear with the ratio of the cavity to the line-shape quality factors as in the case of an active maser [9].

## THE BUFFER GAS

Another important source of frequency shift is the presence of the buffer gas. Even if in principle a buffer gas such as neon can lead to a limiting line width of the order of 40 Hz [3], the practical realization of an atomic frequency standard of interesting medium-and long-term frequency stability puts some constraints on the choice of the buffer gas. In fact, as is well known, one unavoidable effect of the buffer gas is the introduction of a temperature-sensitive frequency shift. However, this temperature sensitivity can be partially compensated by a proper mixture of buffer gases, with opposite temperature coefficients. In practice the use of nitrogen is recommended because of its property of quenching the fluorescence radiation. This radiation is in fact responsible for a loss of coherence in the atomic medium, as it is responsible for the "depumping" processes in the case of classical rubidium standard. A combination of  $N_2$  and of another gas with a negative temperature coefficient is thus preferred. In that case the dark line can be observed only in the transmission mode (bright line). The influence of these buffer gases combined with spin exchange interactions and other broadening mechanisms introduced by the laser light leads to observed line widths of the order of a few hundred hertz and an atomic line  $Q$  of the order of  $2$  to  $3 \times 10^7$ .

## LIMITING SOURCES OF NOISE

Another very important difference between the Dark Line frequency standard and the CPT maser is the limiting source of noise. Since the dark line is observed either through a fluorescence or an absorption signal, its limiting noise is essentially the shot noise plus the additive noise of the background laser radiation. In the case of the maser emission, which is coherent and at microwave frequencies, the noise is of thermal origin [9]. Simple calculation shows that in the CPT maser, the signal-to-noise ratio is proportional to the number of atoms  $N_{\text{atoms}}$ , while in the dark line frequency standard it is proportional to its square root.

$$\begin{aligned} \text{CPT (maser)} \rightarrow \frac{S}{N} &\propto \sqrt{\frac{P_{\text{out}}}{k_B T_B}} \propto \frac{N_{\text{atoms}}}{\sqrt{k_B T_B}} \\ \text{D. L. (freq. stand.)} \rightarrow \frac{S}{N} &\propto \sqrt{N_{\text{atoms}}} + N_{\text{laser}} \end{aligned} \quad (10)$$

## CONCLUSION

In the present paper, the possibility of using the CPT phenomena for the realization of  $^{87}\text{Rb}$  atomic frequency standards has been reviewed. There are two different possible avenues that can be pursued: the use of EIT through the Dark Line approach and the use of the coherent microwave emission through the CPT maser approach. Both avenues are interesting because of their individual characteristics, which are rather different despite their common physical origin.

These proposed frequency standards are both based on the use of the coherence of laser radiation rather than on the use of the laser power as in the case of the classical “intensity pumping” technique. In this sense, the proposed approaches open new avenues with rather promising characteristics.

## REFERENCES

- [1] G. Alzetta, A. Gozzini, L. Moi, and G. Orriols, “An experimental method for the observation of the RF transitions and laser beat resonances in oriented Na vapor,” *Nuovo Cimento B*, 36, 5, 1976.
- [2] A. Godone, F. Levi, and J. Vanier, “Coherent microwave emission in cesium under coherent population trapping,” *Phys. Rev. A*, 59, R 12, 1999.
- [3] J. Vanier, A. Godone, and F. Levi, “Coherent population trapping in cesium: dark lines and coherent microwave emission,” *Phys. Rev. A*, 58, 2345, 1998.
- [4] A. Godone, F. Levi, and J. Vanier, “Coherent Microwave emission without population inversion: a new atomic frequency standard,” *IEEE trans. on I&M*, 504 1999.
- [5] N. Cyr, M. Têtu and M. Breton, *IEEE Trans. Instr. & Meas.*, Vol. 42, 640, 1993.
- [6] A. Godone et al. “Self Consistent Theory of the CPT Maser” (to be published).
- [7] F. Levi, A. Godone, J. Vanier, “The light shift in the coherent population trapping cesium maser,” to appear on *IEEE on UFFC*.
- [8] Patent pending.
- [9] Jacques Vanier and Claude Audoin, “The Quantum Physics of Atomic Frequency Standards,” Adam Hilger, editor, 1989.

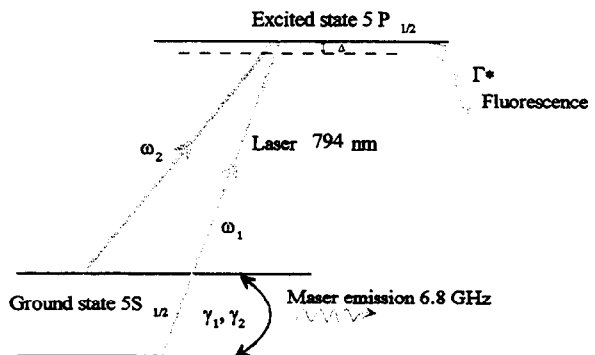


Figure 1 - Scheme of the  $\Lambda$  transition in  $^{87}\text{Rb}$

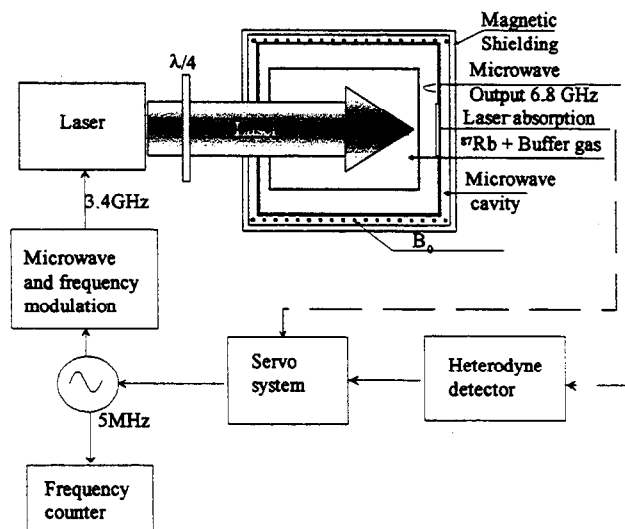


Figure 2 – Experimental set up

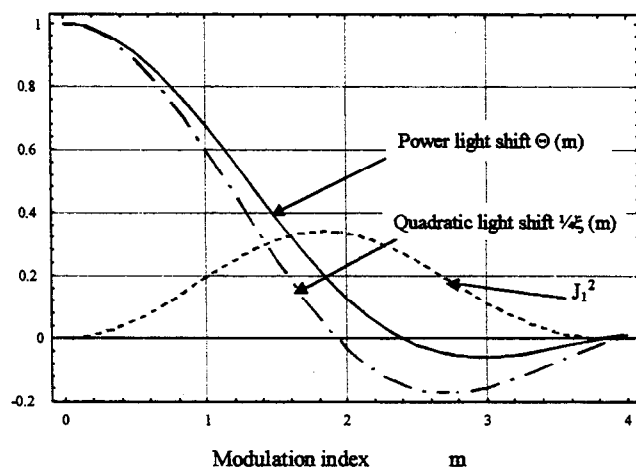


Figure 3- Behavior of the amplitude and frequency light shift in CPT as functions of the frequency modulation index  $m$ .  $J_1^2$  is the relative optical power on the first harmonic when the laser is modulated at half the hyperfine frequency.

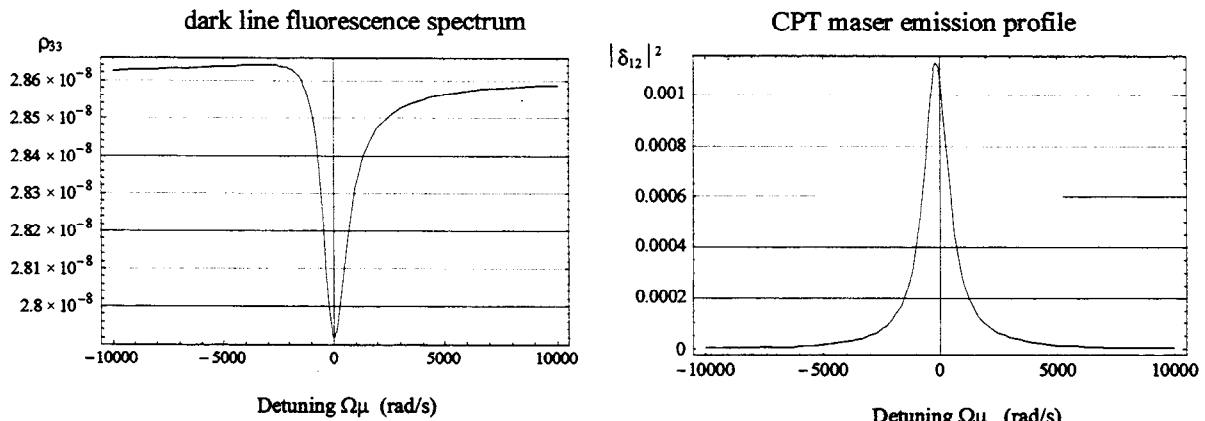


Figure 4 – Mathematical evaluation of the shape of the Dark Line and of the CPT-Maser emission profile with a laser detuning of 300MHz and an asymmetry of 25%, the values of  $\gamma_2$  and  $\Gamma'$  are  $=500 \text{ s}^{-1}$  and  $1060 \text{ s}^{-1}$  respectively.

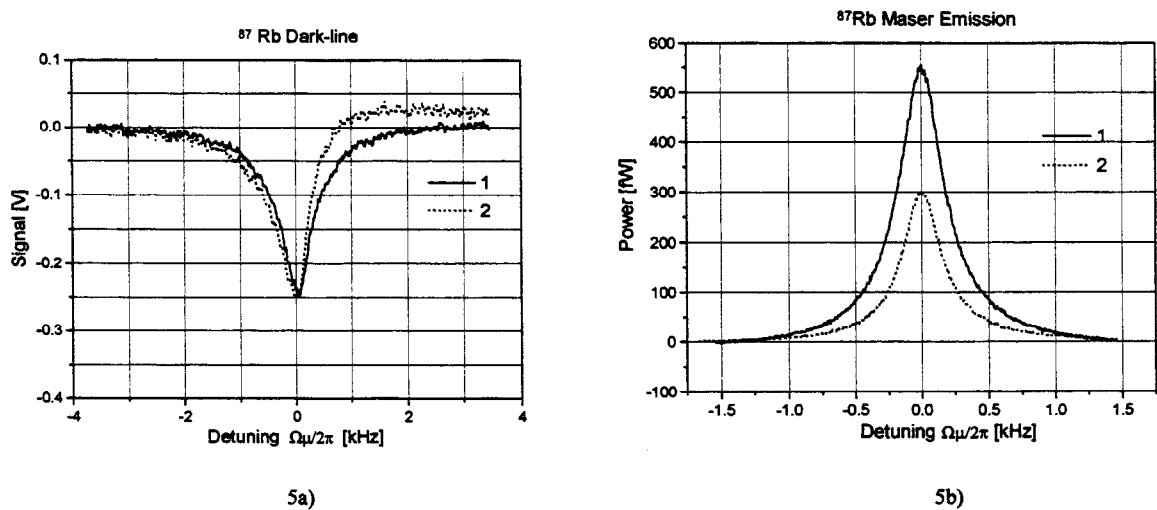


Figure 5 – Experimental data on the asymmetry in the Dark line and in the CPT maser  
 Figure 5a): 1) Laser tuned, asymmetry of 15%; 2) laser detuned by 100 MHz, same asymmetry  
 Figure 5b): 1) laser tuned, excitation symmetric 2) laser detuned by 100 MHz, 50% asymmetry

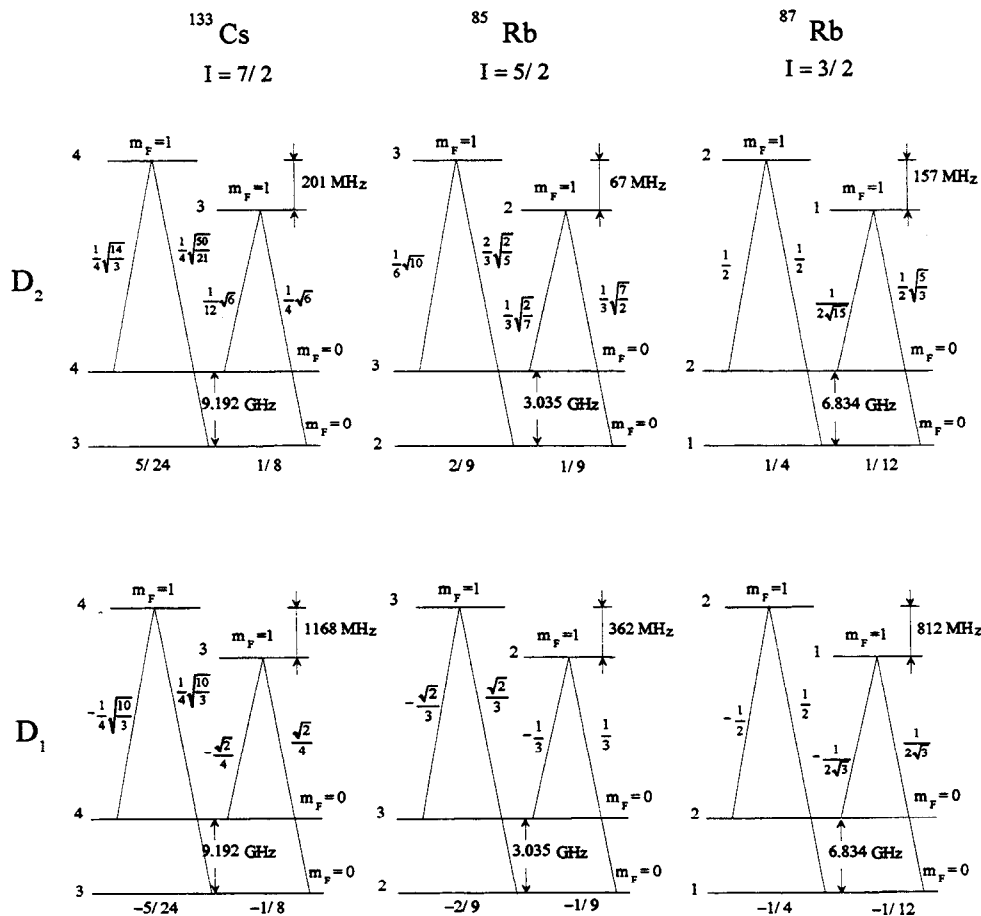


Figure 6 – Values of the electric dipole moments of the transitions used in the excitation of the CPT phenomena in Cs and in both stable isotopes of Rb for D<sub>1</sub> and D<sub>2</sub> lines. In the figures are reported also the values of the hyperfine splitting of the ground state and of the excited state, the nuclear spin, and the relative intensity of each  $\Delta$  transition.